

COMPLEX FIXED-POINT ICA ALGORITHM FOR SEPARATION OF QAM SOURCES USING GAUSSIAN MIXTURE MODEL

Mike Novey and Tülay Adalı

University of Maryland Baltimore County, Baltimore, MD 21250
 {mnovey1, adali@umbc.edu}

ABSTRACT

We introduce a fixed-point algorithm, the complex QAM (C-QAM) algorithm, for separation of quadrature amplitude modulated (QAM) sources through independent component analysis. The algorithm matches the input QAM distribution through a mixture of Gaussian kernels and uses fixed-point updates that fully take advantage of complex domain processing. We demonstrate the performance of the C-QAM algorithm through simulations and note that it provides improved performance over a wide range of operating conditions such as low signal-to-noise ratio, small sample sizes, and large number of sources.

Index Terms— Quadrature amplitude modulation, Nonlinear estimation

1. INTRODUCTION

Independent component analysis (ICA) for separating complex valued signals is needed in many applications such as magnetic resonance imaging, radar, and wireless communications. In this study, we focus on the separation of QAM signals which have found wide use in wireless communications systems using code division multiple access (CDMA). The receivers in these applications are typically quadrature channel, in that at each sample time an in-phase and quadrature-phase value is generated. Thus the signal is inherently complex valued.

In the case of CDMA, multi-user detection may be carried out using several techniques such as matched filters or minimum mean square estimation [1]. More recently, complex-valued ICA has been used to improve CDMA detection by augmenting existing methods as shown in [2], in delay estimation [3], and in interference mitigation [4, 5].

For complex-valued ICA algorithms that use nonlinearities to implicitly generate higher-order statistics such as complex infomax, nonlinear decorrelations, maximum likelihood (ML) [6, 7], and negentropy [8, 9], the optimal choice of nonlinearity is based on the source distribution either through the score function in a likelihood framework, or through entropy in maximization of negentropy. In this study, we use a nonlinearity that matches the joint distribution of a noisy QAM constellation using a mixture of Gaussian kernels. The complex gradient and Hessian of the nonlinearity are derived and are used to develop a complex-valued fixed-point update. Implementing the fixed-point update in the complex domain through a nonlinearity that matches the source distribution, we show leads to a fast and efficient algorithm for QAM source separation.

Tülay Adalı's work was supported by the NSF grants NSF-CCF 0635129 and NSF-IIS 0612076.

2. C-QAM ALGORITHM

2.1. Complex ICA

A complex variable z is defined in terms of two real variables z^R and z^I as $z = z^R + jz^I$. Statistics of a complex random vector $\mathbf{x} = \mathbf{x}^R + j\mathbf{x}^I$ is designated by the joint probability density function (pdf) $p_{\mathbf{x}}(\mathbf{x}^R, \mathbf{x}^I)$. The expectation of a complex random vector \mathbf{x} is then given with respect to this pdf and is written as $E\{\mathbf{x}\} = E\{\mathbf{x}^R\} + jE\{\mathbf{x}^I\}$. A circular random variable is defined as being invariant to rotation, *i.e.*, the pdf of the complex random variable z and $e^{j\alpha}z$ are the same [10] for any α .

In ICA, the observed data \mathbf{z} are typically expressed as a linear combination of latent variables such that $\mathbf{z} = \mathbf{A}\mathbf{s}$ where $\mathbf{s} = [s_1, \dots, s_N]^T$ is the column vector of latent sources, $\mathbf{z} = [z_1, \dots, z_N]^T$ is the column vector of observed mixtures, and matrix \mathbf{A} is the $N \times N$ mixing matrix. We assume that the sources, observations, and mixing matrix are complex valued. ICA then identifies the statistically independent sources given the observed mixtures typically by estimating a matrix \mathbf{W} so that the source estimates become $\mathbf{W}\mathbf{z}$. We assume without loss of generality that the sources have zero mean and unit variance, *i.e.*, $E\{\mathbf{s}\mathbf{s}^H\} = \mathbf{I}$.

2.2. C-QAM cost function

The complex QAM (C-QAM) algorithm we introduce for performing complex ICA of QAM sources, requires a preliminary sphering or whitening transform \mathbf{V} , resulting in

$$\mathbf{x} = \mathbf{V}\mathbf{z} = \mathbf{V}\mathbf{A}\mathbf{s} = \hat{\mathbf{A}}\mathbf{s}$$

where $E\{\mathbf{x}\mathbf{x}^H\} = \mathbf{I}$. Note that $\hat{\mathbf{A}}$, and therefore \mathbf{W} , are unitary as $\mathbf{I} = E\{\mathbf{x}\mathbf{x}^H\} = \hat{\mathbf{A}}E\{\mathbf{s}\mathbf{s}^H\}\hat{\mathbf{A}}^H = \hat{\mathbf{A}}\hat{\mathbf{A}}^H$. Then each source, k , is separately estimated by finding a vector \mathbf{w} such that $y_k = \mathbf{w}_k^H \mathbf{x}$.

C-QAM algorithm is based on maximization of nongaussianity like the FastICA algorithm [11]. As shown in [12], the optimal measure of nongaussianity, based on providing the minimal asymptotic variance estimate, is negentropy defined for a real-valued vector \mathbf{y} as

$$J_{\text{neg}}(\mathbf{y}) = H(\mathbf{y}_{\text{gauss}}) - H(\mathbf{y})$$

where $H(\mathbf{y}) = -E\{\log(p(\mathbf{y}))\}$ is the differential entropy, $p(\mathbf{y})$ is the joint pdf, and $\mathbf{y}_{\text{gauss}}$ is a Gaussian random variable with the same covariance matrix as \mathbf{y} . In the complex case where we have the real and imaginary components of source estimate y_k , we use the 2-D negentropy defined as

$$\begin{aligned} J_{\text{neg}}(y_k^R, y_k^I) &= H(y_{\text{gauss}}^R, y_{\text{gauss}}^I) - H(y_k^R, y_k^I) \\ &= \text{const.} - H(y_k^R, y_k^I) \end{aligned} \quad (1)$$

where $H(y_{\text{gauss}}^R, y_{\text{gauss}}^I)$ is the entropy of a Gaussian random vector and is constant due to the unit variance constraint. We conclude from (1) that maximizing negentropy can be attained by minimizing the 2-D differential entropy $H(y_k^R, y_k^I)$. From (1) we see that when using entropy/nongaussianity as the cost function, the optimal nonlinearity for complex-valued data is

$$J(\mathbf{w}) = E \left\{ \log p_{\text{qam}}(\mathbf{w}^H \mathbf{x}) \right\} \quad (2)$$

where $p_{\text{qam}} : \mathbb{R} \times \mathbb{R} \rightarrow \mathbb{R}$ is the joint pdf of the QAM source to be derived next. We start by noting that for noiseless complex-valued M -QAM sources, the probability mass function (pmf) is

$$p(s) = \begin{cases} \frac{1}{M} & \text{if } s \in \mu \\ 0 & \text{otherwise} \end{cases}$$

where μ is the set of complex points in the constellation, *e.g.*, $\mu = [1, j, -1, -j]^T$ for a 4-QAM source as depicted in Figure 1(a). Our signal model assumes the existence of noise, hence with the addition of complex white Gaussian noise to the sources, a mixture of Gaussian kernels shown in Figures 1(b) and (d) provide a good match to the source distribution. Thus we model the pdf in equation (2) for an M -QAM source with the Gaussian mixture model:

$$p_{\text{qam}}(y) = \frac{1}{M2\pi\sigma^2} \sum_{i=1}^M e^{-\frac{1}{2\sigma^2}((y^R - \mu_i^R)^2 + (y^I - \mu_i^I)^2)}$$

where σ^2 is the variance. The pdf is now a differentiable function which can easily be applied to a gradient-based optimization algorithm.

2.3. C-QAM optimization

Given, the whitened observations \mathbf{x} , we estimate each source, k , separately by finding a vector \mathbf{w} such that

$$y_k = \mathbf{w}_k^H \mathbf{x} = \mathbf{w}_k^H \hat{\mathbf{A}} \mathbf{s} = \mathbf{q}_k^H \mathbf{s} \quad (3)$$

where $\mathbf{q}_k = [0, \dots, q_k, 0, \dots]^T$. Constraining the source estimates such that $E\{y_k y_k^*\} = 1$, also constrains the weights to $\|\mathbf{w}\|^2 = 1$ due to the whitening transform. The optimal weight is then found by maximizing the cost with the unit norm equality constraint given by

$$\mathbf{w}_{\text{opt}} = \arg \max_{\|\mathbf{w}\|^2=1} E\{\log p_{\text{qam}}(\mathbf{w}^H \mathbf{x})\}. \quad (4)$$

From (3), we see that at convergence the optimal solution becomes $\mathbf{q}_{\text{opt}} = [0, \dots, e^{j\theta}, 0, \dots]^T$ indicating that the source estimate is a phase shifted version of the source. This phase shift, as shown in [9], aligns with the distribution of the source. Intuitively, this means that the cost function is maximized when the source is rotated to align with the Gaussian mixture model nonlinearity, *i.e.*, the peaks of the Gaussian mixture model align with the signal constellation (see Figure 1). Thus, the phase ambiguity that exists in complex ICA is alleviated when working within the framework we describe, an important advantage for applications where the phase information is important.

3. FIXED-POINT ALGORITHM

We derive the fixed point algorithm for the constrained optimization problem defined in (4) using a Newton's method based on the Lagrangian function

$$L(\mathbf{w}, \lambda) = J(\mathbf{w}) + \lambda(\mathbf{w}^H \mathbf{w} - 1) \quad (5)$$

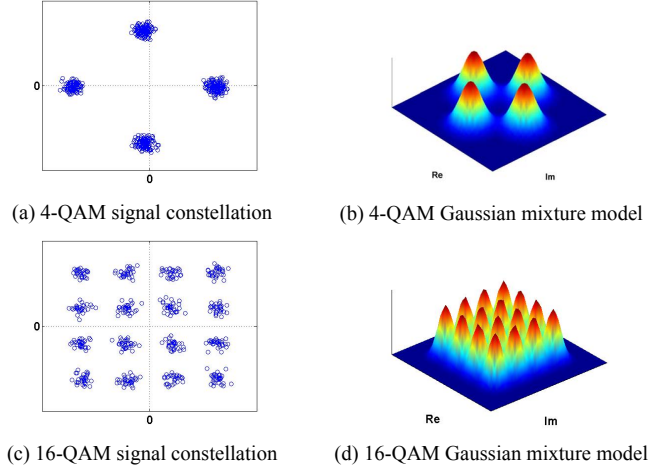


Fig. 1. Signal constellations for 4-QAM and 16-QAM sources with 20-dB SNR along with the Gaussian mixture model in the complex plane.

where λ is the real-valued Lagrange multiplier and J , the cost, is defined in (2).

We make use of the complex gradient and Hessian derived in [13] where the Newton update is defined as

$$\begin{aligned} \Delta \tilde{\mathbf{w}} &= - \left(\frac{\partial^2 f}{\partial \tilde{\mathbf{w}}^* \partial \tilde{\mathbf{w}}^T} \right)^{-1} \frac{\partial f}{\partial \tilde{\mathbf{w}}^*} \\ &= -\mathbf{H}_J^{-1} \tilde{\nabla}_J^* \end{aligned}$$

where \mathbf{H} is the complex Hessian, $\tilde{\nabla}^*$ is the conjugate gradient and complex vectors, denoted with a tilde, are of the form $\tilde{\mathbf{z}} \in \mathbb{C}^{2N} = [z_1, z_1^*, \dots, z_N, z_N^*]^T$. The Newton update to the Lagrangian (5) is written as

$$\Delta \tilde{\mathbf{w}} = -(\mathbf{H}_J + \lambda \mathbf{I})^{-1} (\tilde{\nabla}_J^* + \lambda \tilde{\mathbf{w}}^n)$$

and upon expanding we obtain

$$(\mathbf{H}_J + \lambda \mathbf{I}) \tilde{\mathbf{w}}^{n+1} = -\tilde{\nabla}_J^* + \mathbf{H}_J \tilde{\mathbf{w}}^n \quad (6)$$

where $\Delta \tilde{\mathbf{w}} = \tilde{\mathbf{w}}^{n+1} - \tilde{\mathbf{w}}^n$. The conjugate gradient, $\tilde{\nabla}_J^*$, derived in the Appendix is

$$\tilde{\nabla}_J^* = 1/2E \{ \mathbf{x} g^*(y) \}$$

where $y = \mathbf{w}^H \mathbf{x}$. The complex Hessian, also derived in the Appendix, is given by

$$\mathbf{H}_J = E \left\{ \begin{bmatrix} x_1 x_1^* g_a'(y) & x_1^2 g_b'(y) & \dots \\ (x_1^2)^* g_b'^*(y) & x_1 x_1^* g_a'(y) & \dots \\ \vdots & \vdots & \ddots \\ x_N x_1^* g_a'(y) & x_N x_1 g_b'(y) & \dots \\ (x_N^2)^* g_b'^*(y) & x_N x_1^* g_a'(y) & \dots \end{bmatrix} \right\}.$$

We write \mathbf{H}_J the sum of two matrices, $\mathbf{H}_J = \mathbf{H}_J^a + \mathbf{H}_J^b$, where

$$\mathbf{H}_J^a = E \left\{ \begin{bmatrix} x_1 x_1^* g_a'(y) & 0 & x_1 x_2^* g_a'(y) & \dots \\ 0 & x_1^* x_1 g_a'(y) & 0 & \dots \\ \vdots & \vdots & \vdots & \ddots \end{bmatrix} \right\}$$

and

$$\mathbf{H}_J^b = E \left\{ \begin{bmatrix} 0 & x_1 x_1 g_b'(y) & 0 & \dots \\ x_1^* x_1^* g_b'^*(y) & 0 & x_1^* x_2 g_b'^*(y) & \dots \\ \vdots & \vdots & \vdots & \ddots \end{bmatrix} \right\}$$

to rewrite the product $\mathbf{H}_J \tilde{\mathbf{w}}$ as

$$\mathbf{H}_J \tilde{\mathbf{w}} = \mathbf{H}_J^a \tilde{\mathbf{w}} + \mathbf{H}_J^b \tilde{\mathbf{w}}. \quad (7)$$

Expanding (7) and simplifying by retaining the non-conjugated values or odd-numbered rows results in

$$\mathbf{H}_J \mathbf{w} = E \left\{ \mathbf{x} \mathbf{x}^H g'_a(y) \right\} \mathbf{w} + E \left\{ \mathbf{x} \mathbf{x}^T g'_b(y) \right\} \mathbf{w}^* \quad (8)$$

with $\mathbf{H}_J \mathbf{w} \in \mathbb{C}^N$. Substituting (8) into (6) and making use of the approximation, $E\{x_i x_j f(y)\} \approx E\{x_i x_j\} E\{f(y)\}$, and the whiteness of \mathbf{x} we obtain

$$\mathbf{K} \mathbf{w}^{n+1} = -1/2 E\{\mathbf{x} g(y)\} + E\{g'_a(y)\} \mathbf{w}^n + E\{\mathbf{x} \mathbf{x}^T\} E\{g'_b(y)\} (\mathbf{w}^n)^* \quad (9)$$

where $\mathbf{K} = (\mathbf{H}_J + \lambda \mathbf{I})$. How well the approximation $E\{x_i x_j f(y)\} \approx E\{x_i x_j\} E\{f(y)\}$ is satisfied depends on the function $f(\cdot)$ and the data statistics. In the cases we studied, the difference $|E\{x_i x_j f(y)\} - E\{x_i x_j\} E\{f(y)\}| < \gamma$ where $\gamma = 10\sigma_x^2$ initially and $\gamma \rightarrow 0$ as the algorithm iterates since then $y = \mathbf{w}^H \mathbf{x} \rightarrow s_i$.

At the convergence point, \mathbf{K} becomes real valued, as shown in [14], and can be removed from the due to the subsequent normalization of \mathbf{w} to unit norm. Our fixed-point update now becomes

$$\mathbf{w}^{n+1} = -1/2 E\{\mathbf{x} g(y)\} + E\{g'_a(y)\} \mathbf{w}^n + E\{\mathbf{x} \mathbf{x}^T\} E\{g'_b(y)\} (\mathbf{w}^n)^*.$$

4. SIMULATIONS

We verify the performance of the C-QAM algorithm presented in this paper first using 4-QAM sources and then 16-QAM sources with added white complex Gaussian noise as depicted in Figure 1. We measure the performance at various signal to noise ratios (SNR) as the number of samples and number of sources are adjusted. We test the performance of C-QAM against joint approximate diagonalization of eigenmatrices (JADE) [15] and complex FastICA (C-FastICA) [8] with nonlinearity $G(y) = \log(.1 + |y|^2)$. We also compare performance with a more recent fixed-point algorithm (C-FP) proposed in [16] that showed promising performance for this type of problem. The C-FP algorithm uses a nonlinearity based on kurtosis and takes into account the noncircular nature of the sources. For C-QAM, C-FastICA, and C-FP, we implement symmetric orthogonalization such that all sources are estimated in parallel and the demixing matrix is orthogonalized using $\mathbf{W} \leftarrow (\mathbf{W} \mathbf{W}^H)^{1/2} \mathbf{W}$. We noted slightly better results using symmetric orthogonalization rather than using the deflationary mode. For C-QAM, in these simulations, we we did not pursue adapting the variance, σ^2 , to the sources but chose a fixed value of .5 for 4-QAM and .2 for 16-QAM.

The performance of the algorithms are measured using the intersymbol interference index (ISI), quantifying the distance of the permutation matrix $\mathbf{P} = \mathbf{W} \mathbf{A}$ from the optimum, defined as

$$\text{ISI}(\mathbf{P}) = \frac{1}{N} \sum_{i=1}^N \left[\sum_{k=1}^N \frac{|P_{ik}|}{\max_k |P_{ik}|} - 1 \right]$$

where the lower the ISI value the better the separation with zero defining perfect separation. The results are averaged over 100 runs with the mixing matrix and realizations of the sources recalculated on each run.

Figures 2 and 3 depict the performance of the algorithms with ten 4-QAM and ten 16-QAM sources respectively. The number

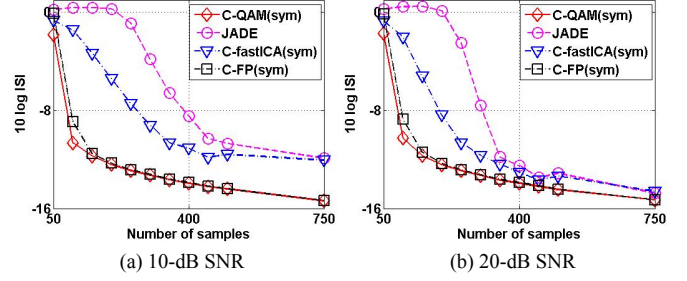


Fig. 2. ISI vs. number of samples for 10-dB and 20-dB SNR levels with 4-QAM sources.

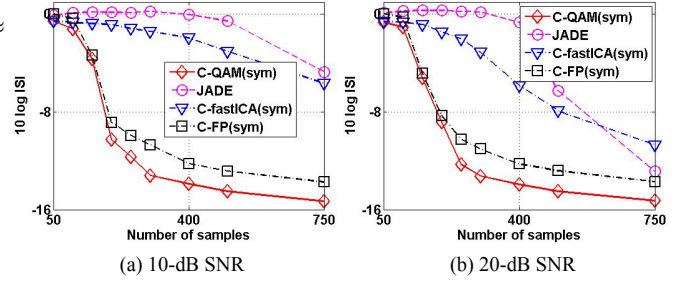


Fig. 3. ISI vs. number of samples for 10-dB and 20-dB SNR levels with 16-QAM sources.

of samples is varied from 50 to 750 at SNR levels of 10-dB and 20-dB. We observe that C-QAM significantly outperforms JADE and C-FastICA at both SNR levels as seen in Figure 2. We see a more modest improvement, about 1-dB, against C-FP specifically with small sample sizes and low SNR levels with 4-QAM sources. However C-QAM significantly outperforms all algorithms with 16-QAM sources as seen in Figure 3. This seems to indicate that explicitly matching the nonlinearity to the source distribution provides substantial improvement over non-matching nonlinearities such as kurtosis.

Figure 4 depicts the performance of the algorithms as the number of sources is varied from 5 to 30 at SNR levels of 10-dB (a) and 20-dB (b). Again we observe that C-QAM provides improved performance, in this case, by extending the usable range of operation as the number of sources grow.

5. CONCLUSIONS

In this paper, we presented the C-QAM algorithm for separation of QAM signals in a noisy environment. We derived a fixed-point algorithm in the complex domain using a Gaussian mixture model for the nonlinearity. We show that explicitly matching the nonlinearity to the QAM source distribution provides improved performance, even when confronted with low SNR signals, small sample sizes, or a large number of sources.

A. APPENDIX

We make use of the complex gradient

$$\frac{\partial f}{\partial z} = \frac{1}{2} \left(\frac{\partial f}{\partial z^R} - j \frac{\partial f}{\partial z^I} \right); \quad \frac{\partial f}{\partial z^*} = \frac{1}{2} \left(\frac{\partial f}{\partial z^R} + j \frac{\partial f}{\partial z^I} \right) \quad (10)$$

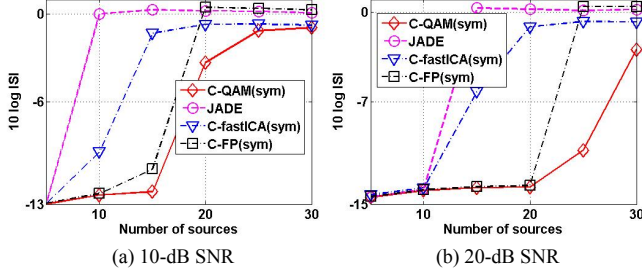


Fig. 4. ISI vs. number of 4-QAM sources with different SNR levels (400 samples).

and Hessian

$$\nabla_{\mathbf{z}}^2 f(\mathbf{z}_0) = \left. \frac{\partial^2 f(\mathbf{z})}{\partial \mathbf{z}^* \partial \mathbf{z}^T} \right|_{\mathbf{z}=\mathbf{z}_0} \quad (11)$$

for non-analytic functions as defined in [13] where complex vectors are of the form $\mathbf{z} = [z_1, z_1^*, \dots, z_N, z_N^*]^T$.

The complex gradient of (2) is found by applying (10) and the chain rule to find the partial derivative

$$\begin{aligned} \frac{\partial J(\mathbf{w})}{\partial w_i^*} &= \frac{1}{2} E \left\{ \frac{\partial \log p_{\text{qam}}(\mathbf{w}^H \mathbf{x})}{w_i^R} + j \frac{\partial \log p_{\text{qam}}(\mathbf{w}^H \mathbf{x})}{w_i^I} \right\} \\ &= \frac{1}{2} E \left\{ \left(g^R(y) \frac{\partial(\mathbf{w}^H \mathbf{x})^R}{\partial w_i^R} + g^I(y) \frac{\partial(\mathbf{w}^H \mathbf{x})^I}{\partial w_i^R} \right) + \right. \\ &\quad \left. j \left(g^R(y) \frac{\partial(\mathbf{w}^H \mathbf{x})^R}{\partial w_i^I} + g^I(y) \frac{\partial(\mathbf{w}^H \mathbf{x})^I}{\partial w_i^I} \right) \right\} \end{aligned}$$

where

$$\begin{aligned} g^R(y) &= \frac{\partial \log p_{\text{qam}}(y)}{\partial y^R} = \frac{-1}{M 2\pi \sigma^4 p_{\text{qam}}(y)} \sum_{i=1}^M (y^R - u_i^R) e^{\gamma(y)}, \\ g^I(y) &= \frac{\partial \log p_{\text{qam}}(y)}{\partial y^I} = \frac{-1}{M 2\pi \sigma^4 p_{\text{qam}}(y)} \sum_{i=1}^M (y^I - u_i^I) e^{\gamma(y)}, \end{aligned}$$

and $\gamma(y) = \frac{-1}{2\sigma^2} [(y^R - u_i^R)^2 + (y^I - u_i^I)^2]$. Noting that

$$\begin{aligned} \frac{\partial(\mathbf{w}^H \mathbf{x})^R}{\partial w_i^R} &= x_i^R & \frac{\partial(\mathbf{w}^H \mathbf{x})^R}{\partial w_i^I} &= x_i^I \\ \frac{\partial(\mathbf{w}^H \mathbf{x})^I}{\partial w_i^R} &= x_i^I & \frac{\partial(\mathbf{w}^H \mathbf{x})^I}{\partial w_i^I} &= -x_i^R \end{aligned} \quad (12)$$

we find

$$\begin{aligned} \frac{\partial J(\mathbf{w})}{\partial w_i^*} &= \frac{1}{2} E \left\{ g^R(y) x_i^R + g^I(y) x_i^I + j \left(g^R(y) x_i^I - g^I(y) x_i^R \right) \right\} \\ &= \frac{1}{2} E \{ x_i g^*(y) \} \end{aligned} \quad (13)$$

where the last line uses complex notation.

The complex Hessian is similarly found by applying (10) and (11) to (2). Starting with (13), we find the second derivative

$$\begin{aligned} \frac{\partial^2 J(\mathbf{w})}{w_i^* w_k} &= \frac{1}{4} E \left\{ x_i \left[\frac{\partial(g^R(y) - j g^I(y))}{\partial w_k^R} - j \frac{\partial(g^R(y) - j g^I(y))}{\partial w_k^I} \right] \right\} \\ &= \frac{1}{4} E \left\{ x_i \left[x_k^R (g^{RR} + g^{II}) + x_k^I (g^{RI} - g^{IR}) + \right. \right. \\ &\quad \left. \left. j \left(x_k^R (g^{RI} - g^{IR}) - x_k^I (g^{RR} + g^{II}) \right) \right] \right\} \\ &= \frac{1}{4} E \left\{ x_i x_k^* \left[g^{RR} + g^{II} + j (g^{RI} - g^{IR}) \right] \right\} \\ &= E \left\{ x_i x_j^* g'_a \right\} \end{aligned}$$

where we used (12) and define

$$\begin{aligned} g^{RR} &\equiv \frac{\partial g^R(y)}{\partial y^R} = (g^R(y))^2 + \sum_{i=1}^M \frac{e^{\gamma(y)}}{M 2\pi p_{\text{qam}}(y)} \left[\frac{-1}{\sigma^4} + \frac{(y^R - u_i^R)^2}{\sigma^6} \right] \\ g^{II} &\equiv \frac{\partial g^I(y)}{\partial y^I} = (g^I(y))^2 + \sum_{i=1}^M \frac{e^{\gamma(y)}}{M 2\pi p_{\text{qam}}(y)} \left[\frac{-1}{\sigma^4} + \frac{(y^I - u_i^I)^2}{\sigma^6} \right] \\ g^{IR} &\equiv g^{RI} = \frac{\partial g^R(y)}{\partial y^I} = g^R(y) g^I(y) + \sum_{i=1}^M \frac{(y^R - u_i^R)(y^I - u_i^I)}{M 2\pi \sigma^6 p_{\text{qam}}(y)} e^{\gamma(y)} \end{aligned}$$

and $g'_a \equiv 4[g^{RR} + g^{II} + j(g^{RI} - g^{IR})]$. Using similar steps we find

$$\begin{aligned} \frac{\partial^2 J}{\partial w_i^* \partial w_j} &= E \{ x_i x_j^* g'_a \} & \frac{\partial^2 J}{\partial w_i^* \partial w_j^*} &= E \{ x_i x_j g'_b \} \\ \frac{\partial^2 J}{\partial w_i \partial w_j} &= E \{ x_i^* x_j^* g'_a \} & \frac{\partial^2 J}{\partial w_i \partial w_j^*} &= E \{ x_i x_j^* g'_a \} \end{aligned}$$

where $g'_b = 4[g^{RR} - g^{II} + j(g^{RI} + g^{IR})]$.

B. REFERENCES

- [1] S. Verdú, *Multiuser Detection*, Cambridge University Press, 1998.
- [2] T. Ristaniemi and J. Joutsensalo, "Advanced ICA-based receivers for DS-CDMA systems," in *Proc. IEEE PIMRC*, London, September 18-21 2000.
- [3] R. Cristescu, T. Ristaniemi, J. Joutsensalo, and J. Karhunen, "Delay estimation in CDMA communications using a FastICA algorithm," in *In Proc. ICA Workshop*, 2000.
- [4] T. Ristaniemi, K. Raju, and J. Karhunen, "Jammer mitigation in DS-CDMA array system using independent component analysis," in *In Proc. IEEE Int. Conf. on Communications*, New York, April 2002.
- [5] K. Raju and J. Sarela, "A denoising source separation based approach to interference cancellation for DS-CDMA array systems," in *In Proc. 38th Asilomar Conference on Signals, Systems and Computers*, Pacific Grove, USA, Nov. 7-10 2004.
- [6] T. Adali, T. Kim, and V. Calhoun, "Independent component analysis by complex nonlinearities," in *Proc. ICASSP*, Montreal, Canada, May 2004, vol. 5, pp. 525-528.
- [7] J.-F. Cardoso and T. Adali, "The maximum likelihood approach to complex ICA," in *Proc. ICASSP*, Toulouse, France, May 2006.
- [8] E. Bingham and A. Hyvarinen, "A fast fixed-point algorithm for independent component analysis of complex valued signals," *Int. J. Neural Systems*, vol. 10, pp. 1-8, 2000.
- [9] M. Novey and T. Adali, "ICA by maximization of nongaussianity using complex functions," in *Proc. MLSP*, Mystic, CT, 2004.
- [10] B. Picinbono, "On circularity," *IEEE Trans. Signal Processing*, vol. 42, pp. 3473-3482, Dec. 1994.
- [11] A. Hyvärinen, "Fast and robust fixed-point algorithms for independent component analysis," *IEEE Transactions on Neural Networks*, vol. 10, no. 3, pp. 626-634, 1999.
- [12] A. Hyvärinen, "One-unit contrast functions for independent component analysis: a statistical analysis," in *Proc. IEEE Workshop*, Sep. 1997, pp. 388-397.
- [13] A. van den Bos, "Complex gradient and Hessian," in *IEE Proc. Image Signal Processing*, Dec. 1994, vol. 141, pp. 380-382.
- [14] M. Novey and T. Adali, "Adaptable nonlinearity for complex maximization of nongaussianity and a fixed-point algorithm," in *Proc. MLSP*, Maynooth, Ireland, Sept. 2006.
- [15] J.-F. Cardoso and A. Souloumiac, "Blind beamforming for non-gaussian signals," in *IEE Proc. Radar Signal Proc.*, 1993, vol. 140, pp. 362-370.
- [16] S. Douglas, "FastICA algorithms for the blind separation of complex-valued signal mixtures," in *Proc. Asilomar Conf. Signals, Systems and Computers*, October 2005, pp. 1320-1325.